Application of compatibility-based stress fields for the quantification of minimum shear reinforcement

Aplicación de campos de tensiones considerando compatibilidad de deformaciones para la cuantificación de la armadura mínima de cortante

Jaime Mata-Falcón[*, a], Marius Weber[b] and Walter Kaufmann[c]

[a] Dr. Civil Engineer. ETH Zurich, Switzerland. Senior Assistant. mata-falcon@ibk.baug.ethz.ch

[b] Dr. Civil Engineer. ETH Zurich, Switzerland. Postdoctoral Researcher. weber@ibk.baug.ethz.ch

[c] Dr. Civil Engineer. ETH Zurich, Switzerland. Chair of Structural Engineering. kaufmann@ibk.baug.ethz.ch

[*] Corresponding author

ABSTRACT

The Compatible Stress Field Method (CSFM) is a computer-aided FE-based stress field design, in which classical stress fields are complemented with kinematic considerations and more refined material constitutive relationships. Among other benefits, this allows accounting for tension stiffening to capture closely the load-deformation behaviour of the elements. This work explores the capability of the CSFM to predict stirrup failures caused by insufficient ductility, showing that the minimum shear reinforcement amount prescribed by current structural concrete codes might be insufficient to prevent this brittle failure for large beam depths and reinforcing steels of low and normal ductility classes.

RESUMEN

El 'Compatible Stress Field Method' (CSFM) es una herramienta informática de diseño mediante campos de tensiones basada en el MEF, en la cual las hipótesis clásicas de campos de tensiones se complementan con consideraciones de compatibilidad. Esto permite, entre otros beneficios, implementar el efecto de tension-stiffening necesario para capturar adecuadamente la deformabilidad en servicio y rotura. Este trabajo explora las posibilidades del CSFM para predecir fallos de la armadura de cortante por insuficiente ductilidad, mostrando que la armadura mínima de cortante actualmente prescrita podría ser insuficiente para evitar este modo de fallo frágil en vigas de gran canto y ductilidad media y baja de las armaduras.

KEYWORDS: limit analysis, stress fields, shear, minimum reinforcement, deformation capacity
PALABRAS CLAVE: análisis límite, campos de tensiones, cortante, armadura mínima

1. Introduction

Strut-and-tie models and stress fields are popular methods for the design, dimensioning and detailing of concrete structures, particularly suitable for the so-called *discontinuity regions*, where Bernoulli's hypothesis of plane sections remaining plane is inappropriate and hence, design cannot be based on sectional analysis.

Both are lower-bound limit analysis methods based on the theory of plasticity. Under the assumption of a perfectly plastic material behaviour, the lower-bound theorem of limit analysis can be formulated as: "Every loading for which it is possible to specify a statically admissible stress state that does not infringe the

yield condition is not greater than the ultimate load." [1]. Therefore, lower-bound limit analysis methods, and strut-and-tie models and stress fields in particular, provide a safe estimation of the ultimate load of the structure allowing the designer to freely choose the resistance mechanism.

A key aspect in the application of limit analysis to structural concrete is the consideration of perfectly plastic material behaviour, which requires the structural element to have enough deformation capacity to develop the plastic redistributions required by the assumed stress state. Hence, only if this requirement is satisfied the theorems of limit analysis are valid, and stress fields and strut-and-tie models can be considered lower bounds for the ultimate load. Pioneers in the application of the theory of plasticity to reinforced concrete like Nielsen and Thürlimann and his co-workers, were fully aware of the limited ductility of concrete and even reinforcement. They performed extensive investigations into the deformation capacity of structural concrete to determine the limits of applicability of limit analysis methods [2–7], whose results are partly reflected in current design codes, e.g. through limits for moment redistribution in hyperstatic girders, bounds for the inclination of the compression field, minimum reinforcement and rules for the effective concrete compressive strength.

Classical stress field solutions have been reviewed in the recent years to allow for computer-aided structural design [8–10]. These new solutions consist in FE-implementations including kinematic considerations, which allow for the automatic generation of optimum stress fields. They open the way for more efficient stress field analysis, particularly when the effective concrete compressive strength is computed automatically by using compression softening relationships. The load-deformation behaviour can also be estimated provided refined material constitutive relationships accounting for tension stiffening are considered, as done in the Compatibility Based Stress Field Method (CSFM) presented in Section 2. This work explores the capability of the CSFM to verify the deformation capacity, namely to predict stirrup failures caused by insufficient ductility, which cannot be captured when using classic lower-bound solutions according to limit analysis (e.g. strut-and-tie models and stress fields) nor elastic-perfectly plastic automated stress field analyses. The minimum shear reinforcement required to avoid brittle failures of the stirrups in 3-point bending tests is quantified in Section 4 for different shear slenderness and reinforcement ductilities.

2. Compatible Stress Field Method

2.1 Scope

The Compatible Stress Field Method (CSFM) is a method for computer-aided stress field design that allows an automatic design and assessment of structural concrete members subjected to in-plane loading, i.e. beams, walls and, particularly, discontinuity regions. The following information is a summary of the descriptions in [10,11]. The CSFM consists of a continuous, FE-based 2D stress field analysis in which the classical stress field solutions are complemented with kinematic considerations and more refined material constitutive relationships. This allows (i) computing the effective compressive strength of concrete automatically based on the state of transverse strain, similarly as in compression field analyses accounting for compression softening [2,12] and the Elastic Plastic Stress Field method [9]) and (ii) accounting for tension stiffening to capture closely the load-deformation behaviour of the elements. Aiming to foster the use of computer-aided stress fields by structural engineers, the CSFM has been implemented in *IDEA StatiCa Detail*, a new user-friendly commercial software developed jointly by ETH Zurich and the software company IDEA StatiCa.
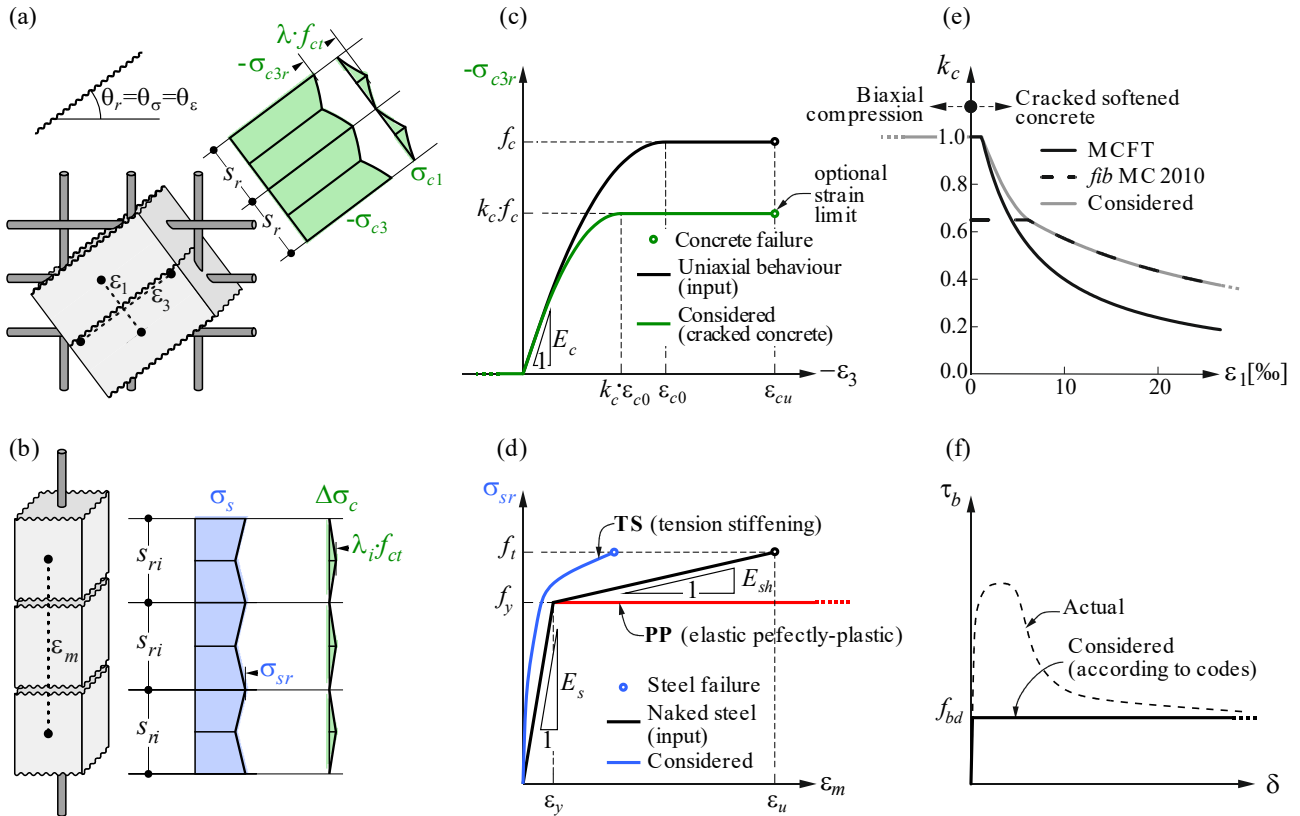
Figure 1. Basic assumptions of the CSFM model: (a) principal stresses in concrete and reinforcement; (b) stresses in the reinforcement direction; (c) stress-strain diagram of concrete in terms of maximum stresses and considering compression softening; (d) stress-strain diagram of reinforcement in terms of stresses at the cracks and average strains; (e) compression softening law; (f) bond shear stress-slip relationship for anchorage length verifications.

2.2 Main assumptions and limitations

The CSFM assumes fictitious, rotating, stress-free cracks opening without slip (Figure 1a) and considers the equilibrium at the cracks together with average strains of the reinforcement. Hence, the model considers maximum concrete (σ_{c3r}) and reinforcement stresses (σ_{sr}) at the cracks, while it neglects the concrete tensile strength ($\sigma_{c1r}=0$) except for its stiffening effect on the reinforcement (Figure 1b,d). This is consistent with classic concrete design.

With these assumptions, the principal directions of stresses and strains coincide and the behaviour of the principal directions in the cracked state is decoupled except for the compression softening effect (Figure 1e). This justifies the use of the simple uniaxial laws presented in the following sections.

It should be noted that, similarly to classical strut-and-tie models and stress fields, the CSFM is not suitable for designing slender elements without transverse reinforcement. Structural elements analysed by the CSFM should always contain a minimum ratio of transversal reinforcement to avoid potential brittle failures.

2.3 Constitutive models

2.3.1. Concrete

The concrete model in the CSFM is based on the uniaxial compression laws prescribed by design codes for cross sectional design, which only depend on the compressive strength. This study considers the parabola-rectangle diagram from EN 1992-1-1 [13] (Figure 1c), assuming a perfectly plastic branch (i.e. no concrete strain limit in compression is considered).

The effective compressive strength is automatically evaluated for cracked concrete based on the principal tensile strain (ε_1) by means of the k_c reduction factor, as shown in Figure 1c-e. The implemented compression softening relationship (Figure 1e) is a generalisation of the *fib* Model Code 2010 [14] proposal for shear verifications. The relationship proposed in the Modified Compression Field Theory [2] (plotted as well in Figure 1e), or similar ones, lead to much stronger softening for large tensile strains. A possible reason for this divergence is that the fitting of this compression softening relationship included experimental results with reinforcement failures (i.e. the relationship does not cover exclusively the compression softening effect) [15]. While these differences are irrelevant in the CSFM (the reinforcement fails still in the range with moderate divergences in the compression softening value), they might be critical in models not capturing the failure of the reinforcement.

2.3.2. Reinforcement

The bare (unbonded) reinforcement is idealised by the bilinear stress-strain diagram contained in design codes (black line in Figure 1c). This is perfectly defined based on the strength and ductility class of the reinforcement.

The CSFM accounts for tension stiffening by modifying the stress-strain relationship of the reinforcing bare steel (unbonded) in order to capture the average stiffness of the bars embedded in concrete (ε_m, blue line in Figure 1c). This default approach in CSFM (referred to as "TS" in this study) will be compared in Sections 3 and 4 to an elastic perfectly plastic idealization without accounting for tension stiffening (referred to as "PP" in this study).

The CSFM also allows verifying the anchorage length of the reinforcement, by introducing a simplified bond-shear stress slip relationship between the concrete and the reinforcement (Figure 1f); however, this study assumes perfect anchorage.

2.3.2. Tension stiffening

The tension-stiffening model distinguishes between stabilised and non-stabilised crack patterns. In both cases, concrete is considered fully cracked before loading (i.e. concrete tensile strength is neglected for equilibrium).

In fully developed crack patterns, tension stiffening is introduced using the Tension Chord Model (TCM) [4,6] – Figure 2a. The TCM assumes a stepped, rigid-perfectly plastic bond shear stress-slip relationship with $\tau_b = \tau_{b0} = 2f_{ctm}$ for $\sigma_s \leq f_y$ and $\tau_b = \tau_{b1} = f_{ctm}$ for $\sigma_s > f_y$. Treating every reinforcing bar as a tension chord (see Figure 1b-d and Figure 2a), the distribution of bond shear, steel and concrete stresses and hence the strain distribution between two cracks can be determined for any given value of the maximum steel stresses (or strains) at the cracks. The application of the TCM depends on the reinforcement ratio and, hence, assigning an appropriate concrete area acting in tension between the cracks to each reinforcing bar is crucial. This is done automatically in the CSFM by using a procedure to define the corresponding effective reinforcement ratio (ρ_{eff}) for any reinforcement configuration. Details of this procedure can be found elsewhere [10,11].

Cracks existing in regions with geometric reinforcement ratios lower than ρ_{cr}, i.e. the minimum reinforcement amount for which the reinforcement is able to carry the cracking load without yielding, are generated by either non-mechanical actions (e.g. shrinkage) or progression of cracks controlled by other reinforcement. The value of this minimum reinforcement is given in Equation (1):

$$\rho_{cr} = \frac{f_{ct}}{f_y - (n-1)f_{ct}} \tag{1}$$

where f_y = reinforcement yield strength; f_{ct} = concrete tensile strength; and $n = E_s / E_c$ = modular ratio. For conventional concrete and reinforcing steel ρ_{cr} amounts to around 0.6%. It should be noted that ρ_{cr} is

approximately sevenfold the minimum amount of shear reinforcement prescribed by current design concrete codes [13,14]:

$$\rho_{w,min} = \frac{0.08 \cdot \sqrt{f_c}}{f_{yw}} \qquad (2)$$

where f_{yw} = stirrups yield strength and f_c = concrete compressive strength.

For stirrups with reinforcement ratios below ρ_{cr}, (i.e. in most practical cases), cracking is considered as non-stabilised and tension stiffening is implemented by means of the Pull-Out Model (POM) [10] described in Figure 2b. This model analyses the behaviour of a single crack by (i) considering no mechanical interaction between separate cracks, (ii) neglecting the deformability of concrete in tension and (iii) assuming the same stepped, rigid-perfectly plastic bond shear stress-slip relationship used by the TCM. This allows

obtaining the reinforcement strain distribution (ε_s) in the vicinity of the crack for any maximum steel stress at the crack (σ_{sr}) directly from equilibrium. Given the fact that the crack spacing is unknown in a non-fully developed crack pattern, the average strain (ε_m) is computed for any load level over the distance between points with zero slip when the reinforcing bar reaches its tensile strength (f_t) at the crack ($l_{\varepsilon,avg}$ in Figure 2b). This is an indirect assumption for the crack spacing that has proven to give reasonable estimations of the serviceability behaviour [16] and the load bearing capacity of elements with low amounts of shear reinforcement [10,11], including members with stirrups failures due to insufficient ductility.

The behaviour including tension stiffening for the most common European reinforcing steel (B500B, with $f_t/f_y = 1.08$ and $\varepsilon_u = 5\%$) is illustrated in Figure 2c-d.
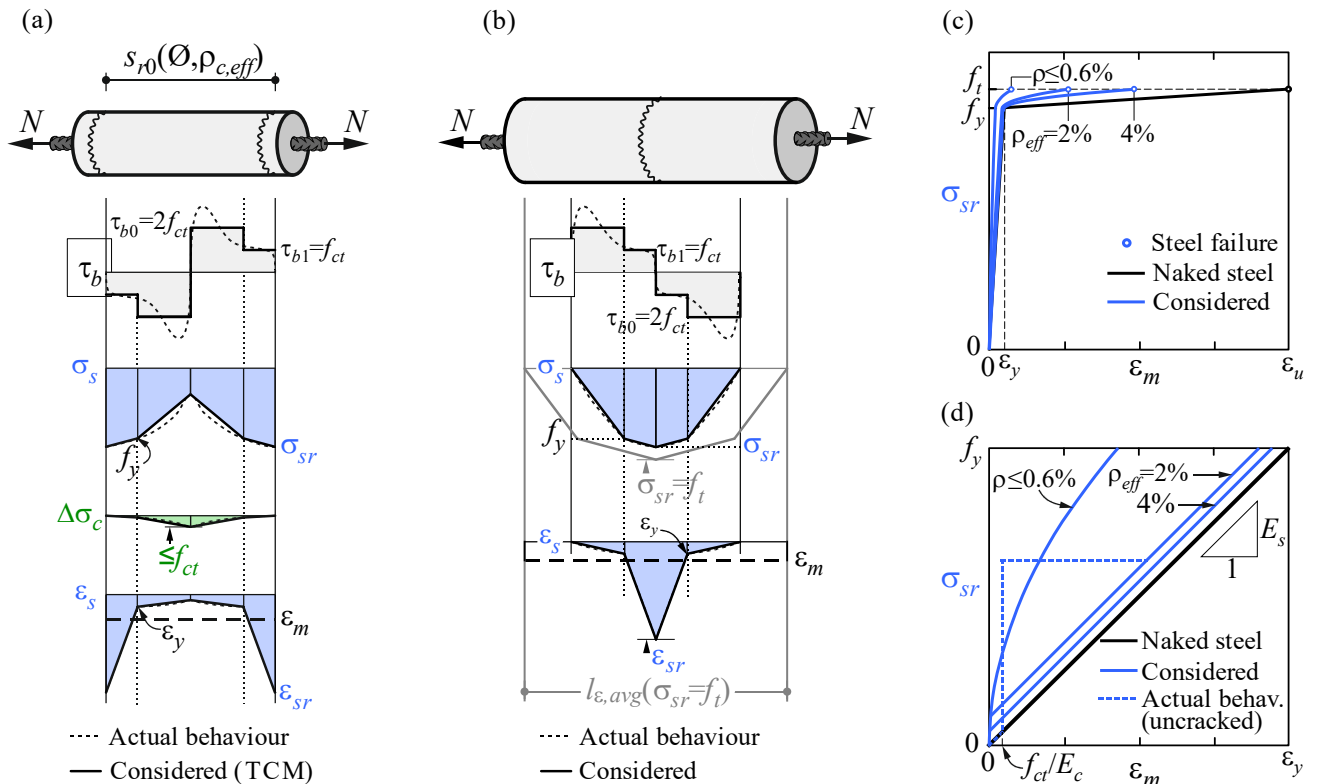
Figure 2. Tension-stiffening model: (a) tension chord element for stabilised cracking with distribution of bond shear, steel and concrete stresses, and steel strains between cracks; (b) pull-out assumption for non-stabilised cracking with distribution of bond shear and steel stresses and strains around the crack; (c) resulting tension chord behaviour in terms of reinforcement stresses at the cracks and average strains for European B500B steel; (d) detail of the initial branches of the tension chord response.

3. Experimental validation

This section presents an experimental validation of the CSFM in beams with (i) low amounts of shear reinforcement (i.e. around the current minimum amount prescribed, $\rho_{w,min}$ acc. Eq. (2)), and (ii) large beam depths. The specimens with shear reinforcement from the experimental campaign of Huber et al. [17] are selected to this end. Figure 3 and Table 1 describe the geometry, test setup and reinforcement layout of the tests.

The material properties used in the numerical analysis have been directly extracted from the measured experimental material properties [17], and can be found elsewhere [11]. The ductility of the stirrups complies with class A according to EN 1992-1-1 [13]. In all four beam experiments, the failure was triggered by the rupture of the stirrups.

Table 1. Shear reinforcement of the validation tests.

Specimen	ρ_w [%]	s_t [mm]	$\emptyset_t$ [mm]
R500m351	0.094	200	6
R500m352	0.084	200	4
R1000m60	0.094	400	12
R1000m35	0.094	200	6
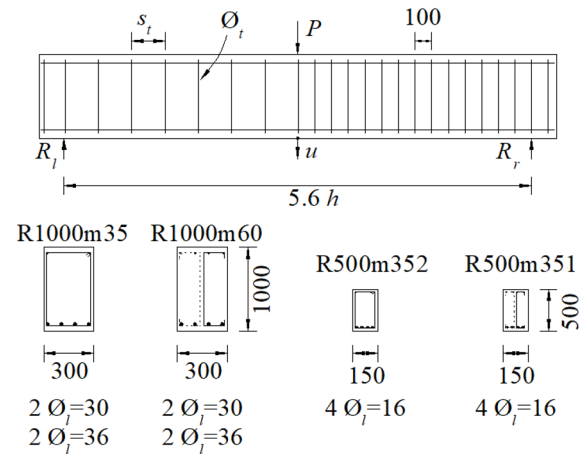
Figure 3. Experimental setup of the validation tests [mm].
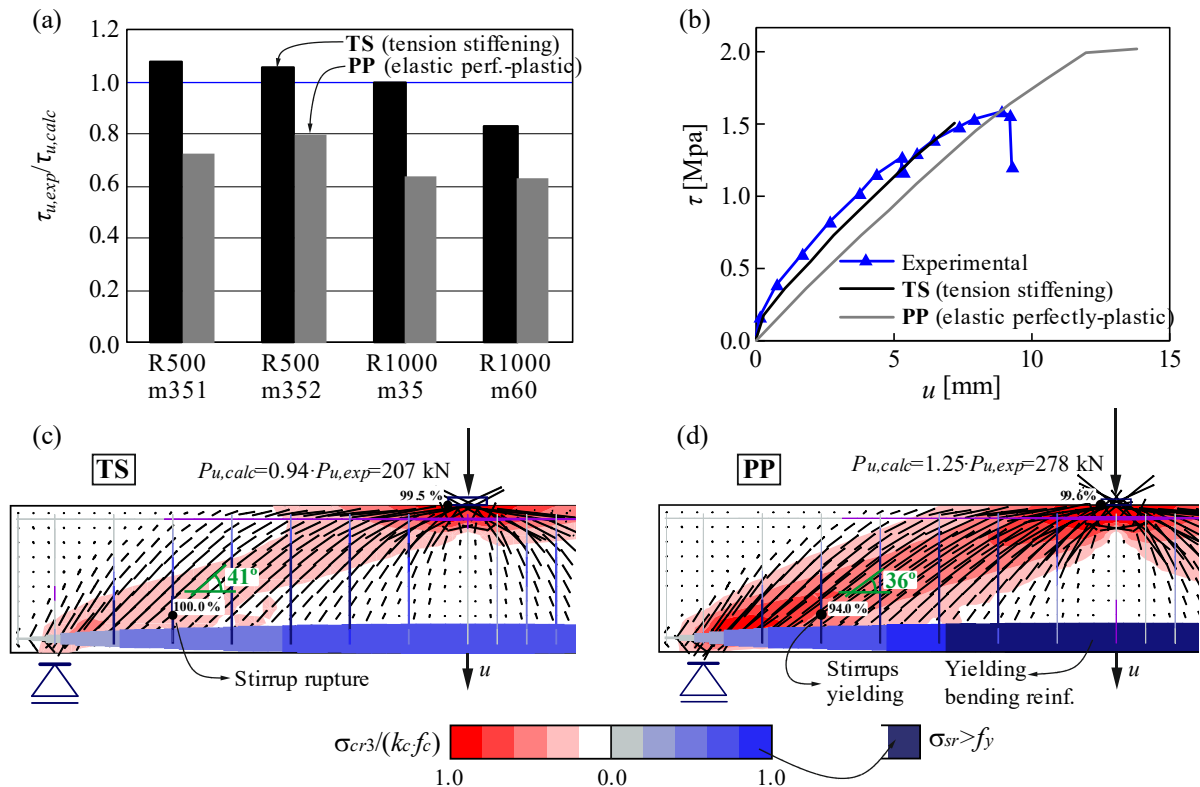
Figure 4. Numerical results for R-Series of Huber et al. [17]: (a) ratio of experimental and predicted load; (b) load-deformation response of R500m352; (c)-(d) compatible stress fields for R500m352, considering tension stiffening (TS) and elastic perfectly plastic reinforcement behaviour (PP).

The numerical model was built discretising the depth of the beams with a total of 10 finite elements. Two constitutive relationships of the reinforcement were compared (see TS vs PP in Figure 1d): a model including tension-stiffening (TS), i.e. verifying the deformation capacity, and an elastic perfectly plastic (PP) idealization of the reinforcement, i.e. assuming sufficient deformation capacity.

The results using the CSFM are shown in Figure 4. The load bearing capacity can be well predicted on average when considering tension (TS) stiffening (Figure 4.a), but the assumption of sufficient deformation capacity (PP) is inappropiate: it overestimates the load bearing capacity by 25…60% (43% on average). The experimental failure mode (stirrup failures), is well predicted in all tests when considering tension stiffening (TS), but the elastic-perfectly plastic reinforcement idealization (PP) leads always to bending failures with yielding of the longitudinal reinforcement (see e.g. Figure 4.d). The load deformation response of beam R500m352 (Figure 4.b) shows that the perfectly plastic model is excesively soft for service loads and mismatches the shear failure mode. If stirrups yield but do not fail, the shear strength can still be further increased as a flatter inclination of the compression field can be achieved (compare the inclinations shown in Figure 4.c and d). Therefore, if the failure of the stirrups is not modelled, the numerical model will either fail in bending or due to concrete crushing in the web (or both simultaneously).

While relying on the web concrete crushing to capture indirectly the load bearing capacity in members with potential brittle failure of the stirrups (by using a pronounced compression softening expression) is an approach followed by some models, the results presented in this section show that this might be significantly unsafe, specially in large depth beams (representative of real-life structures) and low reinforcement ductilities. Such approaches are sensitive to the selected compression softening relationship. Moreover, it is mechanically inconsistent, as key aspects in such failures (e.g. reinforcement ductility and amount) cannot be captured. The consideration of tension stiffening allows capturing properly such failures and provides reasonable estimations of the deformation capacity.

4. Quantification of minimum shear reinforcement

This section extends the observations concerning the resistance overestimation when sufficient deformation capacity is presumed to a wider range of parameters. To do so, the virtual experiment in Figure 5 is analysed in the CSFM veryfying (TS) or not (PP) the deformation capacity, similarly as in Section 3. A beam with large constant depth is analysed for 5 shear slendernesses, 5 amounts of shear reinforcement (from 1 to 5 times $\rho_{w,min}$ acc. Eq. (2), i.e. 0.09%) and low, medium and high ductility class reinforcement according to EN 1992-1-1 [13]. The finite element size in the analysis was set to 115 mm. The results of the analysis are displayed in Table 2, Figures 6 and 7, in terms of the ultimate nominal shear stress $\tau = V/(d \cdot b)$.
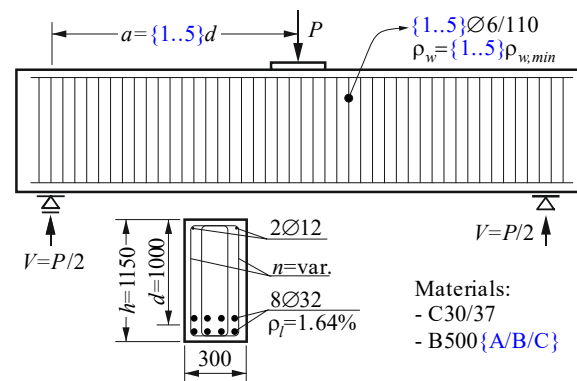
Figure 5. Definition of virtual experiments for quantification of minimum reinforcement. In blue, parameters investigated in the study (dimensions in mm).

Table 2. Load-bearing results for CSFM virtual experiments.

a/d	$\dfrac{\rho_w}{\rho_{w,min}}$	τ_{PP} [MPa]	τ_{TS} [MPa] B500A	B500B	B500C
1.0	1	4.97	4.42	5.05	5.05
1.0	2	5.13	4.88	5.34	5.36
1.0	3	5.26	5.27	5.53	5.54
1.0	4	5.37	5.54	5.68	5.70
1.0	5	5.45	5.81	5.82	5.83
1.5	1	3.88	2.29	3.28	3.99
1.5	2	4.23	2.89	3.88	4.38
1.5	3	4.50	3.39	4.27	4.69
1.5	4	4.72	3.84	4.61	4.96
1.5	5	4.92	4.24	4.91	5.19
2.0	1	2.91	1.53	2.16	2.94
2.0	2	3.47	2.10	2.78	3.48
2.0	3	3.83	2.61	3.33	3.91
2.0	4	4.14	3.07	3.80	4.32
2.0	5	4.37	3.49	4.20	4.52
2.5	1	2.54	1.25	1.66	2.30
2.5	2	3.05	1.84	2.33	2.98
2.5	3	3.43	2.36	2.93	3.51
2.5	4	3.43	2.75	3.45	3.60
2.5	5	3.43	3.09	3.53	3.57
3.0	1	2.22	1.13	1.45	1.94
3.0	2	2.83	1.67	2.15	2.73
3.0	3	2.83	2.08	2.68	2.96
3.0	4	2.83	2.44	2.96	2.97
3.0	5	2.84	2.76	2.97	2.97
3.5	1	2.11	1.04	1.35	1.77
3.5	2	2.34	1.52	1.97	2.50
3.5	3	2.41	1.90	2.43	2.48
3.5	4	2.41	2.23	2.48	2.52
3.5	5	2.41	2.51	2.49	2.53
4.0	1	2.03	0.96	1.26	1.67
4.0	2	2.08	1.40	1.82	2.17
4.0	3	2.08	1.76	2.15	2.11
4.0	4	2.08	2.06	2.12	2.16
4.0	5	2.08	2.15	2.14	2.13
4.5	1	1.84	0.90	1.18	1.58
4.5	2	1.84	1.32	1.69	1.89
4.5	3	1.84	1.65	1.87	1.87
4.5	4	1.84	1.88	1.87	1.88
4.5	5	1.83	1.88	1.88	1.88
5.0	1	1.64	0.85	1.11	1.48
5.0	2	1.64	1.24	1.59	1.67
5.0	3	1.64	1.56	1.68	1.68
5.0	4	1.63	1.70	1.68	1.68
5.0	5	1.63	1.70	1.69	1.69

(a)

(b)

(c)
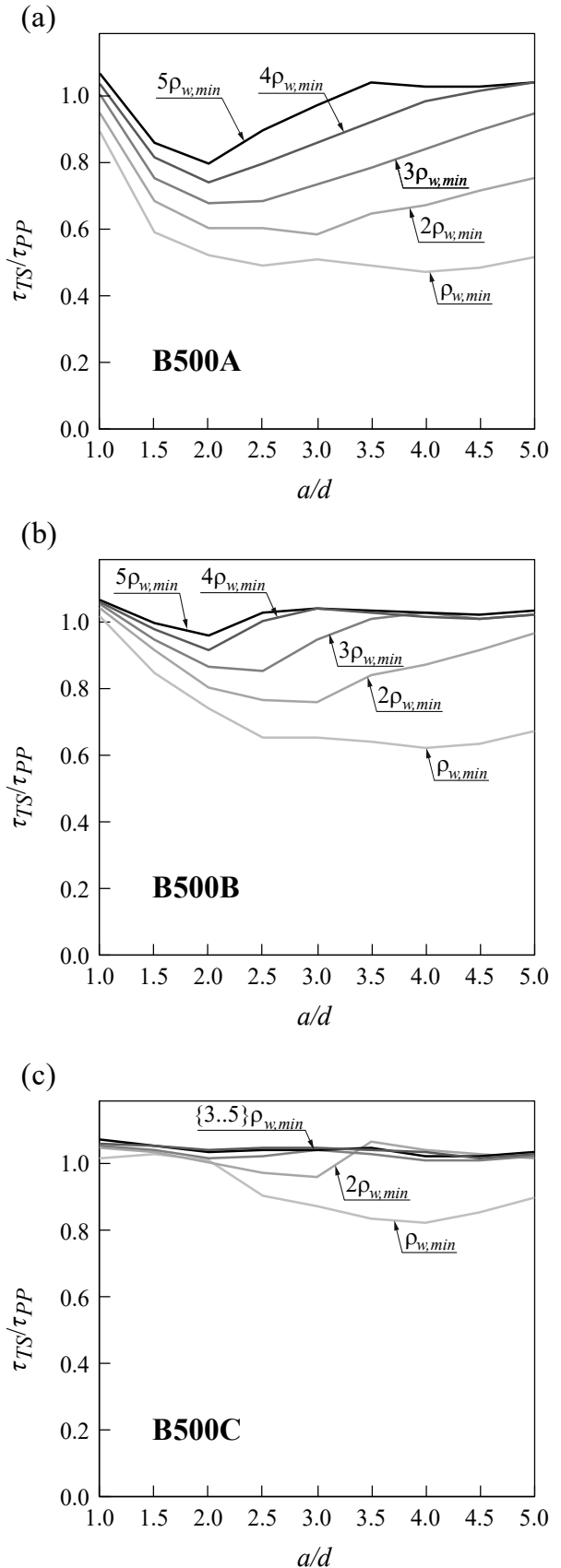
Figure 6. Ratio of shear strength considering deformation capacity (τ_{TS}) over shear strength assuming elastic perfectly plastic behaviour (τ_{PP}): reinforcing steel (a) B500A, (b) B500B and (c) B500C.

This study discusses exclusively the results of ultimate loads of the sensitivity analysis. Based on the results of Section 3, it is assumed that the results of the CSFM including tension stiffening estimate well the bearing capacity of 3-point bending tests with and without failure of the stirrups. In this way, the ratio τ_{TS}/τ_{PP} in Figures 6 and 7 provides an indication of the potential overestimation of the bearing capacity for brittle stirrup failures when presuming sufficient deformation capacity of the reinforcement. Ratios around one indicate that the classical assumption of perfectly plastic behaviour is appropriate, while values clearly below one show that this is unconservative.

Figure 6 shows that the shear slenderness (a/d) around 2.0 is the most prone to brittle stirrup ruptures in the tested configuration. The shape of the curves resembles the 'Kani shear valley' in elements without transverse reinforcement. It can be observed that the valley tends to vanish for low shear slenderness (failure of a direct strut governs) as well as for large shear slenderness (bending failure governs). An increasing amount of transverse reinforcement decreases or eliminates the valley. The results are also highly dependent on the ductility class of the reinforcement, as shown in Figure 7 for the critical shear slenderness. For ductility class C, no issues of insufficient ductility of the reinforcement are expected, and current values of minimum reinforcement are sufficient in this case. Standard ductility class B might require values higher than $\rho_{w,min}$ to ensure a safe application of perfectly plastic models in beams with large depths. Ductility class A should be avoided for plastic analysis without verification of the deformation capacity, as brittle stirrups failures are expected in a wide range of reinforcement amounts.

It should be noted that the results would vary if other stirrup diameters or a different compression softening relationship were considered (see Section 2.3.1), but the general tendencies will remain the same. The aim of this study is merely to emphasise the necessity of further research on shear failures triggered by stirrup ruptures due to their insufficient ductility in large-scale members.
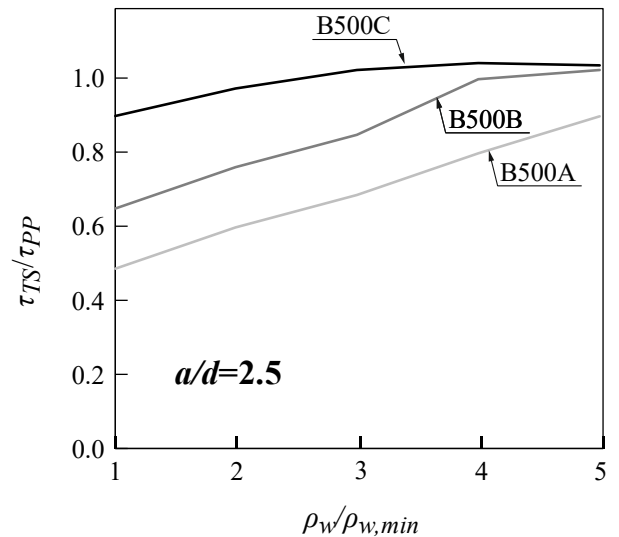
Figure 7. Ratio of shear strength considering deformation capacity (τ_{TS}) over shear strength assuming sufficient deformation capacity (τ_{PP}) for a/d=2.5.

5. Conclusions

This paper has introduced the Compatible Stress Field Method (CSFM), a method for the design and assessment of concrete structures. CSFM is suitable for engineering practice, since it implements simple uniaxial constitutive laws provided in concrete standards. The concrete tensile strength is neglected, but its tension stiffening effect is considered to capture the load-deformation response and the deformation capacity. Experimental failures due to insufficient ductility of the stirrups are shown to be properly captured in the CSFM.

The results show that the minimum reinforcement amount prescribed by current structural concrete codes to ensure a sufficiently ductile behaviour (as little as 0.09% for conventional material properties) might be insufficient to prevent stirrup failures due to insufficient ductility for large beam depths (representative of real-life structures) and reinforcing steels of low and normal ductility classes. Limit analysis solutions presuming sufficient deformation capacity might provide unsafe strength estimations in such cases unless shear reinforcement amounts larger than the current minimum requirements are provided.

References

[1] P. Marti, Theory of structures: fundamentals, framed structures, plates and shells, First edition, Wiley Ernst & Sohn, Berlin, Germany, 2013.

[2] F.J. Vecchio, M.P. Collins, The Modified Compression-Field Theory for Reinforced Concrete Elements subjected to Shear, ACI Structural Journal. 83 (1986) 219–231.

[3] V. Sigrist, Zum Verformungsvermögen von Stahlbetonträgern, PhD Thesis ETH Zurich, Birkhäuser, Basel, 1995.

[4] M. Alvarez, Einfluss des Verbundverhaltens auf das Verformungsvermögen von Stahlbeton, PhD Thesis ETH Zurich, Birkhäuser, Basel, 1998.

[5] W. Kaufmann, Strength and Deformations of Structural Concrete Subjected to In-Plane Shear and Normal Forces, PhD Thesis ETH Zurich, Birkhäuser Basel, Basel, 1998.

[6] P. Marti, M. Alvarez, W. Kaufmann, V. Sigrist, Tension Chord Model for Structural Concrete, Structural Engineering International. 8 (1998) 287–298.

[7] L.C. Hoang, M.P. Nielsen, Plasticity approach to shear design, Cement & Concrete Composites. 20 (1998) 437–453.

[8] C. Sola García, P.F. Miguel Sosa, M.Á. Fenández Prada, Herramienta Informática Avanzada para el Análisis y Diseño de Regiones D en Estructuras de Hormigón, in: IV Congreso ACHE, Valencia, 2008.

[9] M. Fernández Ruiz, A. Muttoni, On development of suitable stress fields for structural concrete, ACI Structural Jorunal. 104 (2007) 495–502.

[10] J. Mata-Falcón, D.T. Tran, W. Kaufmann, J. Navrátil, Computer-aided stress field analysis of discontinuity concrete regions, in: Computer Modeling of Concrete Structures, Proceedingg of the EURO-C Conference, CRC Press, Bad Hofgastein (2018): 641–650.

[11] W. Kaufmann, J. Mata-Falcón, T. Galkovski, D.T. Tran, M. Weber, J. Kabeláč, M. Konecny, J. Navrátil, Compatible Stress Field Design of Structural Concrete: Principles and Validation, in press, 2020.

[12] W. Kaufmann, P. Marti, Structural Concrete: Cracked Membrane Model, ASCE Journal of Structural Engineering. 124 (1998) 1467–1475.

[13] European Committee for Standardization (CEN), Eurocode 2: Design of concrete structures - Part 1-1: General rules and rules for buildings (EN 1992-1-1:2004), Brussels, 2005.

[14] Fédération Internationale du Béton (*fib*), Model Code for Concrete Structures 2010, Ernst & Sohn, Berlin, 2013.

[15] W. Kaufmann, J. Mata-Falcón, A. Beck, Future directions for research on shear in structural concrete, in *fib* Bull. 85: Rational Understanding of Shear in Beams and Slabs (2018) 323-338.

[16] M. Weber, J. Mata-Falcón, K. Thoma, Comparison of crack width predictions by three different models with experimental results on webs of beams, in: Workshop Proceedings No 17, Nordic Concrete Federation, Oslo, 2019: pp. 35–36.

[17] P. Huber, T. Huber, J. Kollegger, Investigation of the shear behavior of RC beams on the basis of measured crack kinematics, Engineering Structures 113 (2016) 41–58.